

2015

X-ray Crystallographic and Functional Characterization of BshC: The Third Step of Bacillithiol Biosynthesis

Andrew VanDuinen
Grand Valley State University

Follow this and additional works at: <https://scholarworks.gvsu.edu/honorsprojects>

 Part of the [Medicine and Health Sciences Commons](#)

ScholarWorks Citation

VanDuinen, Andrew, "X-ray Crystallographic and Functional Characterization of BshC: The Third Step of Bacillithiol Biosynthesis" (2015). *Honors Projects*. 415.
<https://scholarworks.gvsu.edu/honorsprojects/415>

This Open Access is brought to you for free and open access by the Undergraduate Research and Creative Practice at ScholarWorks@GVSU. It has been accepted for inclusion in Honors Projects by an authorized administrator of ScholarWorks@GVSU. For more information, please contact scholarworks@gvsu.edu.

X-ray Crystallographic and Functional Characterization of BshC: The Third Step of Bacillithiol Biosynthesis

Andrew VanDuinen*, and Paul D. Cook*

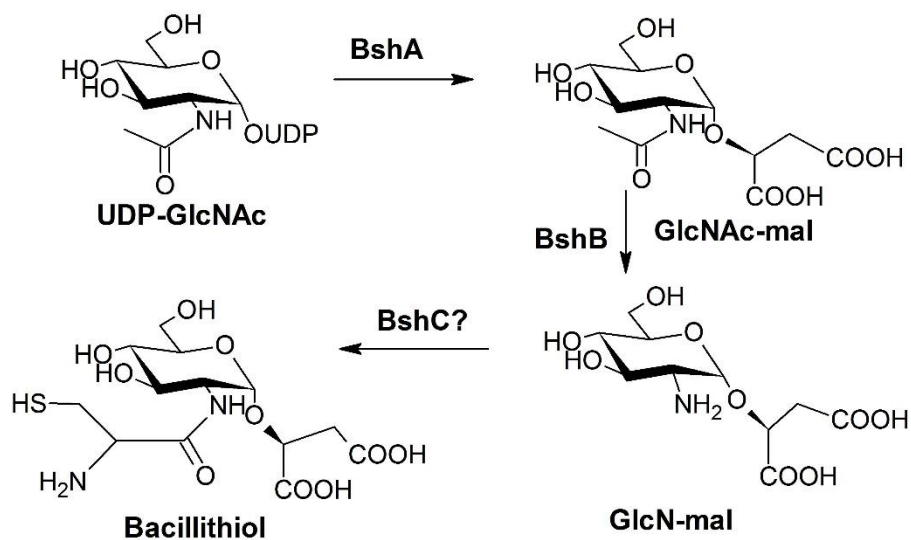
*Department of *Cell & Molecular Biology, Grand Valley State University, Allendale, MI*

Abstract

Bacillithiol is a low molecular weight thiol that reduces oxidative stress and regulates thiol homeostasis in some Gram-positive bacteria, including the pathogenic *Bacillus anthracis* and *Staphylococcus aureus*. It has recently been determined that bacillithiol plays a key role in resistance to the FDA-approved antibiotic fosfomycin. The biosynthesis of BSH is believed to occur via a three step pathway utilizing the enzymes BshA, BshB, and BshC. BshA replaces UDP with malate on UDP-*N*-acetylglucosamine. BshB acts as a deacetylase to produce glucosaminyl-malate, and BshC is proposed to add cysteine to glucosaminyl-malate to produce bacillithiol. The first solved structure of BshC from *Bacillus subtilis* contains three key domains of interest. The first is the active site which putatively adds a cysteine to glucosaminyl-malate. The coiled-coil portion forms a tail-like projection that allows dimerization and is a highly conserved region. The third domain of interest contains an ADP molecule. The function of this domain is highly uncertain, and the amino acid residues are not highly conserved among BshC from various species. *PHYRE2* was used to generate a hypothetical model of BshC from *S. aureus*. The BshC gene was isolated from *S. aureus* genomic DNA. After expressing and isolating the protein, protein crystals will be analyzed via x-ray crystallography to gain insight into the different domains of interest. Functional analysis of BshC will also be pursued to clue into the mechanism dictating its activity. Understanding how BshC functions will allow specific inhibitors to be designed to stop bacillithiol biosynthesis and re-establish fosfomycin as an effective antibiotic once again.

Background and Context

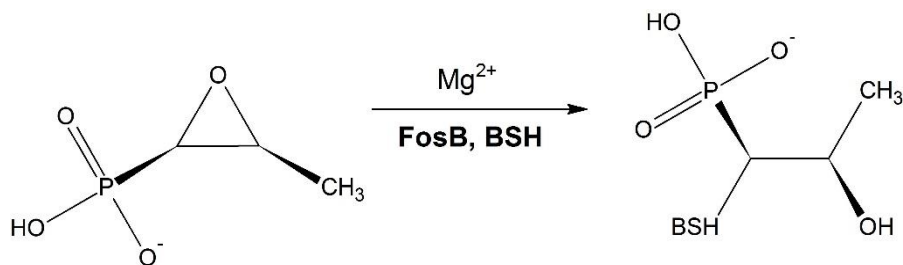
Bacillithiol Cells in an oxidative environment can produce free radicals that damage the cell. For this reason, low molecular weight thiols form disulfide bonds that protect the cell from oxidation. The major low molecular weight thiols include glutathione (GSH), which is found in Gram-negative bacteria, mycothiol (MSH), found in some Gram-positive bacteria, and the recently identified bacillithiol (BSH), also found in Gram-positive bacteria.¹ Bacillithiol (BSH) is classified as a low molecular weight thiol that reduces oxidative stress and regulates thiol homeostasis. It is also capable of detoxifying foreign compounds. BSH is present in many species of *Bacillus* including *B. anthracis*, *B. subtilis*, *B. megaterium*, and is also observed in *Staphylococcus aureus*.² The biosynthesis of BSH is similar to the established pathway of MSH. Using the MSH pathway as a guide, the biosynthesis of BSH was predicted to require three enzymes, BshA, BshB, and BshC in the three step biosynthetic pathway shown in Scheme 1.¹ BshA utilizes malate and UDP-*N*-acetylglucosamine to produce *N*-acetylglucosamine-malate. BshB converts this to glucosamine-malate, and BshC putatively acts as a cysteinyl ligase to convert glucosamine-malate to bacillithiol.



Scheme 1. Bacillithiol biosynthesis pathway.

BSH and Fosfomycin Fosfomycin tromethamine is effective in treating pathogenic *Escherichia coli*, *Citrobacter*, *Enterobacter*, *Klebsiella*, *Serratia*, and *Enterococcus spp.* Taken as a three gram oral dose, it effectively treats urinary tract infections caused by the latter

bacteria.³ Fosfomycin has also been used in combination with other antibiotics to treat the biofilm formation of methicillin-resistant *Staphylococcus aureus* (MRSA).⁴ Bacillithiol can form disulfide bonds between thiols and act as a buffer against alkylating compounds or electrophiles.¹ The FosB enzyme adds BSH to destroy the epoxide ring of fosfomycin conferring resistance to it as depicted in Scheme 2.⁵ Evidence strongly supports BSH as the preferred substrate for this phenomenon.⁶



Scheme 2. Destruction of fosfomycin by FosB utilizing BSH

When the gene encoding BshA, BshB, or BshC is knocked out, BSH production is eliminated; the cell once again becomes sensitive to the antibiotic fosfomycin.⁷ Because of this, inhibitors to any enzyme in the BSH biosynthetic pathway could be designed to re-establish fosfomycin's effectiveness as an antibiotic.

MshC Mechanism. The MshC enzyme from the evolutionarily related mycothiol biosynthetic pathway acts as an ATP-dependent cysteinyl ligase. The intermediate forms an E-AMP-cysteine complex. Prior to binding to the enzyme, ATP binds to cysteine creating an activated cysteine-AMP complex in the active site which then donates cysteine to glucosaminyl-malate.⁸ While BshC has not shown ATP-dependence in *in vitro* studies and has little overlap of amino acid sequence with MshC, the similar Rossmann fold structure of *B. subtilis* BshC to MshC presumably suggests that BshC in fact does function through an activated intermediate complex.

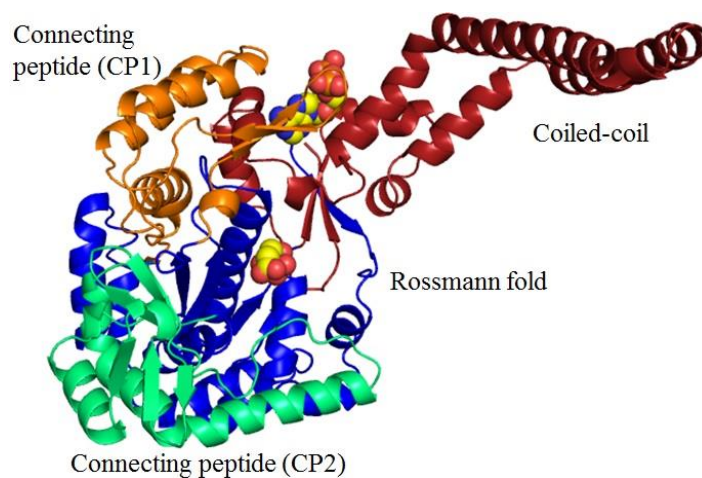


Figure 1. BshC Overall Structure BshC has a core Rossmann fold domain, a coiled-coil tail, connecting peptide region one (CP1), and a connecting peptide region two (CP2).

BshC Structure The overall structure of BshC is depicted in Figure 1. The core Rossmann fold (blue) consists of a beta sheet flanked by two alpha helices. Rossmann folds are able to bind nucleotides and are found in other cysteine ligases such as MshC. The connecting peptide regions flank the core Rossmann fold (green and orange). A unique alpha helical coiled-coil domain (red) projects out as a tail in the monomeric structure.⁹

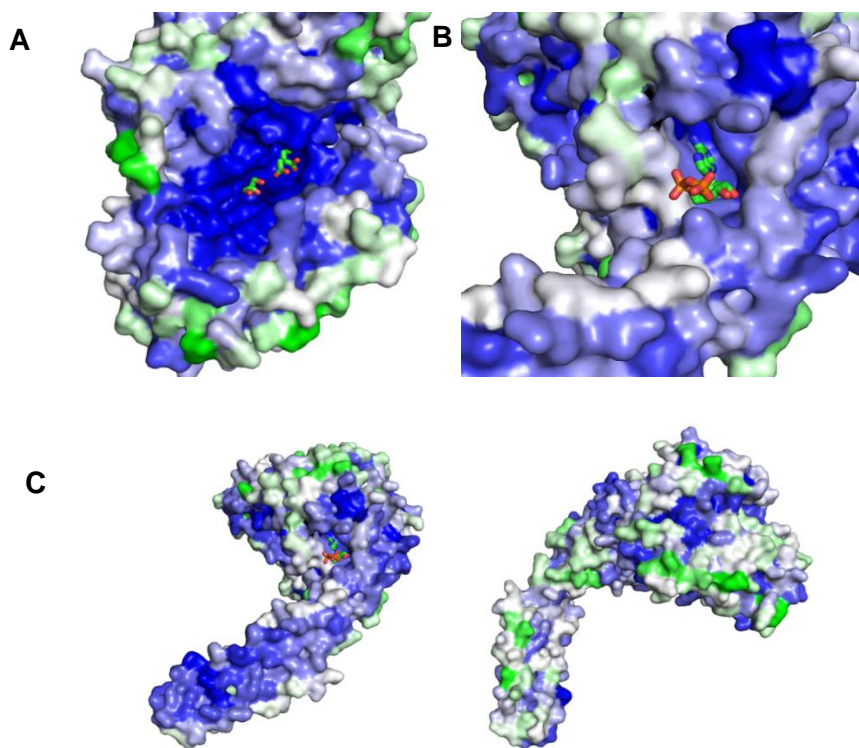


Figure 2. ConSurf Analysis of BshC. Dark blue indicates highly conserved amino acid residues among species. White area indicates amino acid residues not highly conserved among species.

BshC protein from *B. subtilis* overlaid with top BLAST hits in ConSurf shows areas of highly conserved amino acid residues and structure in darker blue and less conserved areas in white. The active site domain is highly conserved among species that produce BSH as shown in Figure 2A by dark blue in the pocket surrounding citrate and glycerol. The coiled-coil domain of BshC, represented as a tail like projection in Figure 2C, also depicts high sequence conservation among species. The domain binding ADP in Figure 2B, however, shows a domain not highly conserved between species as it is lighter blue and more gray. Based on these observations, it is unclear as to whether BshC from other Gram positive species bears amino acid residues that bind ADP in a similar manner as *B. subtilis* BshC does.⁹

In order for a drug to be designed that would be able to bind in the active site and inhibit BshC activity, more information about the active site amino acid residues and the ADP binding pocket is required. A *PHYRE2* model was used to establish a hypothetical structure of BshC from *S. aureus*. Protein crystals will be grown to test this hypothetical structure using x-ray crystallography to enable characterization of *S. aureus* BshC. Functional analysis of BshC was also executed to understand more about the mechanism of its activity. Expanding understanding of the enzyme's structure and function, and the role of ADP in this, will aid in characterizing drugs that inhibit bacillithiol biosynthesis.

Materials and Methods

Overview

PHYRE2 was used to predict the structure of *S. aureus* BshC. To determine the actual structure, the BshC gene was first isolated from *Staphylococcus aureus* genomic DNA. The T7 expression system was used to overexpress BshC protein production using IPTG. The *S. aureus* BshC protein was then purified by Ni-NTA affinity chromatography utilizing the his-tag with solubility and purity being assessed by SDS-PAGE. Pure protein was used to set up crystallization screens and perform functional analysis of BshC.

PHYRE2 Structural Alignment

Protein Homology/Analogy Recognition Engine V 2.0 (*PHYRE2*) was used to map predict a conformational structure of BshC from *S. aureus* based on the known structure of BshC from *B. subtilis*.

Isolation of BshC gene from Staphylococcus aureus genomic DNA.

The BshC gene from *S. aureus* was isolated from total genomic DNA by designing primers 120 and 121 that flank the gene and only replicate BshC in a polymerase chain reaction (PCR). The designed primers contained NheI and XhoI restriction cut sites on their ends so that the isolated gene could be easily manipulated and inserted into the pET-28 expression plasmid. After reconstituting the lyophilized primers and genomic DNA, a 50 uL PCR reaction with 0.5 pmol/uL of each primer and 100 ng of gDNA was carried out with Phusion DNA polymerase from NEB. The result was visualized by agarose gel electrophoresis. DNA was isolated from the gel band by using the GeneJET PCR Purification Kit and DNA concentration determined to be 181ng/uL.

Digestion and Ligation of DNA

Digestion of the PCR DNA with XhoI and NheI was performed with 3.62 ug of DNA so DNA could be ligated into a vector. BshC was ligated into the pET-28 vector using 50 ng of insert and 50 ng of vector in a 10 uL reaction.

E. coli Transformation

About 50 µL of chemically competent *Escherichia coli* cells of the XL-1blue expression strain were incubated on ice with 0.5-4 µL of the BshC pET-28 vector. The mixture rested on ice 10 minutes and was heat shocked at 42°C for 90 seconds. After resting on ice for 6 minutes, the cells were allowed to recover with 250 µL of LB shaking at 200 RPM at 37°C for 1 hour and subsequently plated on LB media containing 25 mg/mL of kanamycin and grown overnight at 37°C.

DNA isolation and Plasmid Digestion

After picking six individual transformed colonies and growing each of them in 5mL of LB overnight, the BshC pET-28 vector was isolated by miniprepping with Thermo Scientific GeneJET Plasmid Miniprep Kit. To confirm the BshC gene was successfully inserted into the plasmid vector, a digestion with NheI and XhoI restriction enzymes was performed on 7 uL of each plasmid and examined by agarose gel electrophoresis. After the BshC gene was shown to be ligated in on an agarose gel, the plasmid was sequenced at the University of Michigan DNA Sequencing Core facility to ensure it was the actual BshC inserted as expected.

Plasmid Propagation

In order to produce more *S. aureus* BshC plasmid DNA for use, 50 μ L of the XL-1Blue expression strain of *E. coli* cells were added to 0.5 μ L of 35 ng/ μ L BshC *S. aureus* in pET-28. After resting on ice for ten minutes, the cells were heat shocked at 42°C for 90 seconds and immediately moved to ice for six minutes. Then, 250 μ L of LB media was added and the tube shaken at 37°C for 45 minutes. After this, the cells were plated onto a 25 mg/mL kanamycin LB agar plate and grown overnight at 37°C. An individual colony was picked and placed in a sterile culture tube containing 7 mL of LB media and 0.25 μ g/mL kanamycin. Four of these tubes were shaken at 200 RPM, 37°C overnight. The next day, the cells were pelleted and miniprepmed using a Thermo Scientific Molecular Biology GeneJET plasmid miniprep kit. The DNA concentration and purity were determined via A₂₆₀ utilizing a Thermo Scientific Nanodrop Spectrophotometer.

Solubility Expression Test

E. coli was transformed with *S. aureus* BshC in pET28 according to “*E. coli* transformation”. A starter culture was used to inoculate 200 mL of LB broth with 25 μ g/ml kanamycin and grown until the OD₆₀₀ reached 0.6. Ni-NTA centrifugation chromatography was used to test protein expression. A 1.02 g cell pellet was re-suspended in 4 mL lysis buffer. Five cycles of 30 sec. of sonication lysed cells and a 100 μ L sample of cell lysate was saved. Lysate was centrifuged 10

min 10,200 RPM at 4°C and a 100 µL supernatant saved. Then, 1 mL of the supernatant was placed in 4 separate 1.5 mL Eppendorf tubes with 200 µL of Ni-NTA resin. The resin was pre-equilibrated 3 times with 1 mL of lysis solution by centrifuging 2 min at 2,000 RPM 4°C and removing supernatant. The loaded supernatant was centrifuged 2 min at 2,000 RPM 4°C. Supernatant was discarded and 1 mL wash buffer added followed by 2 min centrifugation at 2000 RPM 4°C. The wash step was repeated 3 time until close to negative on a Bradford spot test. Then, 100 µL elution buffer was added to the tube and the tube centrifuged 2 min at 10,000 RPM 4°C. The supernatant was then saved as eluate.

Protein Expression

About 50 µL of chemically competent *E. coli* cells of the BL-21 expression strain were incubated on ice with 0.5-4 µL of pET-28 vector containing BshC *S. aureus*. The mixture rested on ice 10 minutes and was heat shocked at 42°C for 90 seconds. After resting on ice for 6 minutes, the cells were allowed to recover with 250 µL LB shaking at 200RPM at 37°C for 1 hour and plated on LB media containing 25 mg/mL of kanamycin and grown overnight at 37°C. Cells were grown in 25 µg/mL kanamycin LB media to 0.6 OD₆₀₀. IPTG was used to induce protein expression and the cells incubated at 16°C overnight with shaking. Cells were harvested by centrifugation at 5500 xg for 25 minutes and stored at -80°C.

Ni-NTA Affinity Chromatography

Recombinant *E. coli* cells with BshC *S. aureus* protein expressed were re-suspended in lysis buffer (20 mM HEPES pH 8, 300 mM NaCl, 10 mM Imidazole). EDTA at 0.5 mM and 0.5 mg/mL of lysozyme were added to digest the cells. MgCl₂ at 5 mM and 5 µg/mL of DNAase were added. The reaction was sonicated. Centrifugation at 17,000 xg for 25 minutes, 4°C was used to isolate the supernatant which was then loaded onto a Pierce HisPur Ni-NTA column equilibrated with lysis buffer. Bradford spot test was used to qualitatively test for the presence of any protein in the column eluate. The column was washed until nearly Bradford negative with wash buffer (20mM HEPES at pH 8, 300mM NaCl, 25mM Imidazole). Samples were then collected, in a single collection vessel, by adding elution buffer (20mM HEPES at pH 8, 300mM NaCl, 250mM Imidazole) to the column until nearly Bradford negative. The collected protein

fractions were dialyzed overnight in dialysis buffer, 20mM HEPES pH 7.5, 50mM NaCl. The procedure was repeated for cell pellet of BshC from *B. subtilis*.

TEV Cleavage

To remove the hexa-histidine tag from the N-terminus of both BshC *B. subtilis* and BshC *S. aureus*, his-tagged protein was dialyzed into Ni-NTA lysis buffer after purification. DTT to 0.5 mM and 1.5 mL of 0.7 mg/mL rTEV in 40% glycerol were added to the sample in dialysis tubing. After dialyzing overnight at room temperature, the protein solution was run down a Ni-NTA column equilibrated with dialysis buffer and collected in fractions. Bradford spot test was run on the flow-through and the column was eluted with 250 mM imidazole buffer after testing nearly Bradford negative. Bradford was used to qualitatively determine purity and efficiency of the TEV cleavage.

Protein Concentration Determination

Dialyzed protein was concentrated by centrifugation in Amicon Ultra-15 Centrifugal Filters and the concentration checked by using a Cary 60 UV-Vis spectrophotometer. The absorbance at 280 nm was measured and the extinction coefficient of 55810 used in Beer's law to determine concentration. Concentrated BshC was frozen in liquid nitrogen and stored at -80°C.

SDS-PAGE

10% SDS-PAGE gels were made by using Amresco instructions and poured 0.75mm thin. Samples of 40 µL from the solubility expression test were prepared for electrophoresis by boiling for five minutes with 2X SDS-PAGE buffer (100 mM tris-HCL pH 6.8, 2%SDS, 4% β-mercaptoethanol, 15% glycerol, 0.2 mg/mL bromothymol blue) in a 1:1 ratio. Electrophoresis was run at 190 V, stained with Coomassie brilliant blue, and destained with 10% MeOH and 10% AcOH in water. Purity was qualitatively assessed.

Crystallization Screens

Crystallization screens were set using the vapor diffusion hanging drop method with Hampton Research Crystal Screen I and II as well as PEG Ion I and II. 400 µL of a condition was placed in

each well. A 12 mg/mL, 2 μ L drop of BshC from *S. aureus* was pipetted on a cover slip and 2 μ L of well solution added to the drop. The slip was inverted over the well with mineral oil forming an air tight seal. Two drops were set up on each cover slip with either 5 mM AMP or apo enzyme. Crystallization screens were also performed on his-tag cleaved BshC *S. aureus* in 5mM cysteine, 2mM BSH with 2mM DTT, or apo conditions.

Functional Analysis of BshC.

To qualitatively analyze BshC activity, *Bacillus subtilis* BshC was added to a BshC substrate reaction containing. The substrate reaction contained 1mM UDP-glcNAc, 1 mM malate, 10 ug BshA, and 10ug of BshB. After reacting for 2 hours at 37°C, 2 mM of cysteine and 5 uL of 2 mg/mL BshC were added to 200 uL assays. To each reaction tube 0.5 mM GTP, 0.5 mM CTP, 0.5 mM ATP, 0.5 mM serine with 0.5 mM ATP, no cysteine with 0.5 mM ATP, 100 uM zinc with 0.5 mM ATP, or 0.5 mM NADH was added. These assay tubes were reacted at 37°C for 30 minutes. Chloroform extraction was performed and the upper aqueous layer saved for HPLC by storing at -20°C. The process was repeated with *S. aureus* BshC with 0.5 mM ATP.

Results and Discussion

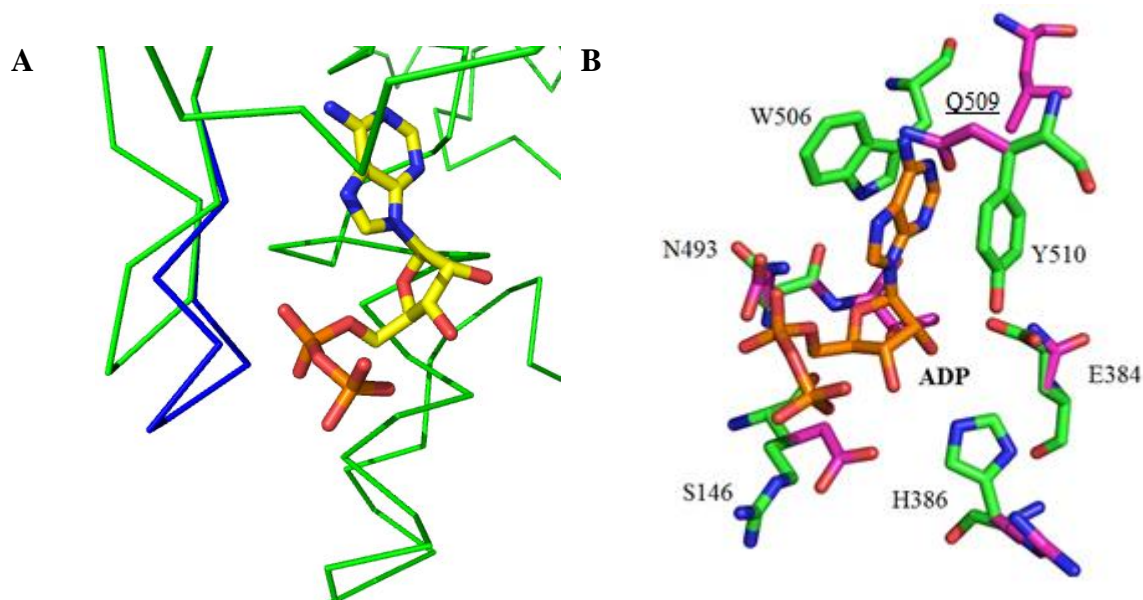


Figure 3. BshC *B. subtilis* ADP Binding Site Compared to PHYRE2 Model of BshC *S. aureus*. (A.) Ribbon structure of *B. subtilis* (green) and model of *S. aureus* (blue) showing extra amino acids in side loop. (B.) Superposition of the ADP binding site in *B. subtilis* structure (green) and *S. aureus* model (magenta).

The PHYRE2 modeling server was used to generate a hypothetical model to predict interactions in the BshC structure from *S. aureus*, specifically in the ADP binding site. The model reported a confidence of 100%. Figure 3A shows a ribbon model of the predicted *S. aureus* model superimposed on the actual *B. subtilis* structure. Two extra amino acids are present in the *S. aureus* protein sequence which results in a larger loop over the ADP binding pocket. Figure 3B depicts superposition of the ADP binding site in *B. subtilis* (green) and *S. aureus* (magenta).

	#	#	#	#	#	#	#
<i>B. subtilis</i>	T ₁₄₅	SE--E ₁₄₈	E ₃₈₄	RHIEKK ₃₉₀	K ₄₈₆	DYERI _{QNS} ₄₉₄	W ₅₀₆ NIMYY ₅₁₁
<i>B. anthracis</i>	V ₁₄₄	TK--N ₁₄₇	E ₃₈₃	RDIATD ₃₈₉	N ₄₈₅	KFRRIQFA ₄₉₃	W ₅₀₅ NVCYY ₅₁₀
<i>B. cereus</i>	V ₁₄₄	AK--N ₁₄₇	E ₃₈₃	RDIATD ₃₈₉	N ₄₈₅	KFRRIQFA ₄₉₃	W ₅₀₅ NVCYY ₅₁₀
<i>S. aureus</i>	A ₁₄₃	YDRIS ₁₄₈	T ₃₈₄	QEAKKC ₃₉₀	R ₄₈₅	HFEIVEHT ₄₉₃	W ₅₀₅ NPIQV ₅₁₀
<i>S. saprophyticus</i>	A ₁₄₃	YNAQN ₁₄₈	Y ₃₈₅	PRTEKL ₃₈₉	K ₄₈₄	HFKEISET ₄₉₂	W ₅₀₄ NPLQI ₅₀₉
<i>S. epidermidis</i>	A ₁₄₃	FNNKE ₁₄₈	Y ₃₈₅	ARTKKL ₃₈₉	R ₄₈₄	QFREISET ₄₉₂	W ₅₀₄ NPLQI ₅₀₉

Figure 4. Multiple sequence alignment of ADP binding pocket residues. The residues of the ADP binding pocket in *B. subtilis* BshC are shown aligned with the BshC sequences of other Firmicutes. Residues from the *B. subtilis* structure that make hydrogen bonding or π -stacking interactions with ADP are indicated with a pound sign (#).

When the amino acid sequences of a few *Bacillus* species are aligned in Figure 4, it is found that residues that interact with ADP are conserved. However, when the sequences of some *Staphylococcus* species are aligned with the *Bacillus* species, they do not contain conserved

residues at the positions that interact with ADP (Figure 4). In Figure 3B, the binding pocket in *B. subtilis* exhibits π -stacking interactions from W506 and Y510. The *PHYRE2* model predicts ADP interactions with the amino acid residues in BshC *S. aureus*. The *S. aureus* ADP binding pocket is predicted to be dissimilar with Q509 present instead of Y510. The Q509 is not able to facilitate π -stacking interactions like Y510 which suggests ADP may not bind as well, if at all. Taken together, this information supports a hypothesis that BshC *S. aureus* might not have an ADP binding site. Nevertheless, *PHYRE2* only predicts the location of amino acid residues and not their exact conformation. A crystal structure is necessary to determine the actual location of the amino acid residues and how they interact with ADP.

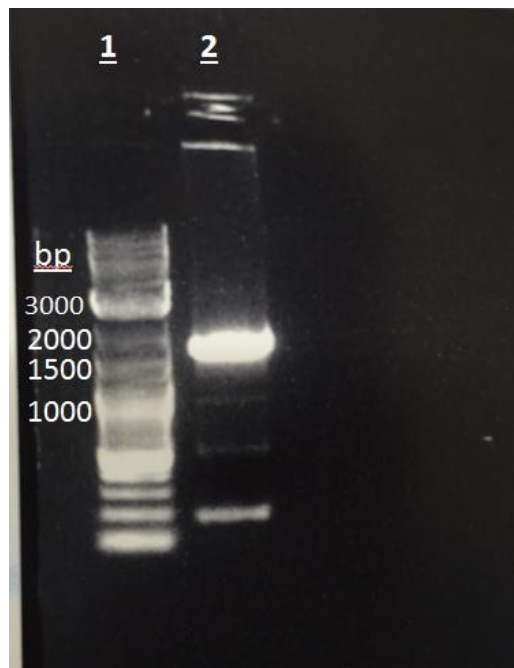


Figure 5. Agarose gel of PCR from *S. aureus* genomic DNA. BshC was amplified by PCR from *S. aureus* genomic DNA. Lane one contains a DNA ladder. Lane 2 contains PCR reaction of BshC gene from *S. aureus* genomic DNA.

PCR product amplified from *S. aureus* genomic DNA was analyzed by agarose gel electrophoresis. The molecular weight DNA ladder in lane one establishes standard MW to determine fragment size. Using the MW ladder in lane one of Figure 5, the BshC gene product in lane two was estimated to be about 1600 bp. This corresponds to the actual BshC gene size suggesting PCR was successful. The small bands in lane two are most likely the 50 bp primers – they just do not resolve well on the 1.5% agarose gel. The PCR product was subsequently

recovered from the gel slice and ligated into the pET-28 vector. *E. coli* cells were successfully transformed with ligation reaction and plated on LB kanamycin plates to select for transformed cells. Because of this, six different colonies were selected and grown overnight in LB kanamycin and the cells miniprepmed to isolate the pET-28 BshC vector.

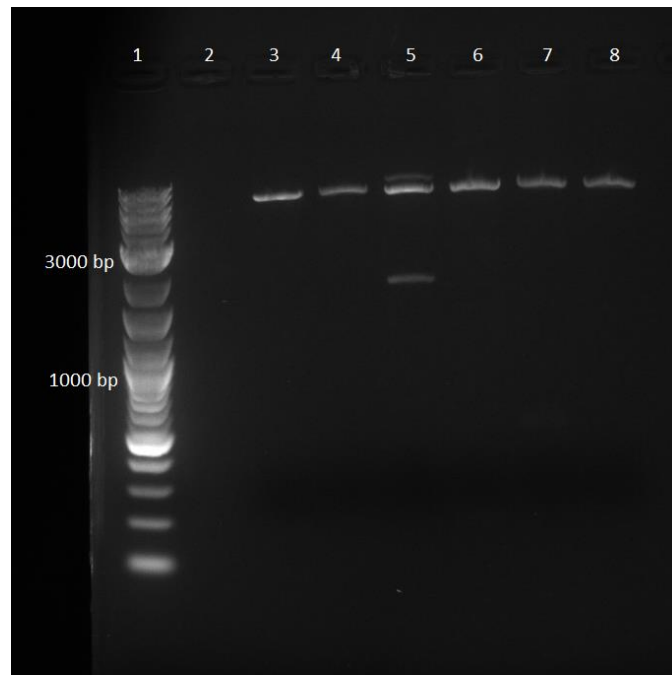


Figure 6. Agarose gel of Plasmid Digestion. Lane one contains DNA ladder. Lane two contains negative control. Lanes three through eight contain the digestion reactions of potential pET28 with BshC insert.

To determine if ligation of BshC into the pET-28 vector was successful, the plasmid DNA from miniprepmed cells was digested with XhoI and NheI restriction enzymes. The result, portrayed in Figure 6, was that only the sample in lane five has BshC successfully ligated into pET-28. The larger band in lane five is the pET-28 vector and the smaller one the gene insert.

The only successful BshC pET-28 vector was sent in for DNA sequencing to confirm the identity of the DNA insert. Figure 7 displays the sequenced DNA aligned with the known sequence of BshC *S. aureus*. The sequence alignment is almost identical, which is expected, except for a few nucleotides near the end of the forward primer because sequencing gets less accurate after 900 bp. The reverse primer accurately overlaps those bases. The alignment confirms the BshC gene was successfully inserted into pET-28. The chromatograms from both the forward and reverse DNA sequencing reactions have been included in the appendix for reference.

CLUSTAL 2.1 multiple sequence alignment

```

BshCFwd      CGTGGGAATTCCCTCTGAATATTTGTTTACTTTAAGAAGGAGATATACCATGGGCAGCA 60
BshCaureus   -----
BshCFwd      GCCATCCCTCNCTCATCATCACAGCAGCGAGAACCCTGTACTTCCAGGGCCATATGGCTAGC 120
BshCaureus   -----
BshCFwd      ATGGACTGTAAAGTAGTTAGTTTAAATGAAAAAGATCAGTTTATACCAAAAAATAAGAGC 180
BshCaureus   ATGGACTGTAAAGTAGTTAGTTTAAATGAAAAAGATCAGTTTATACCAAAAAATAAGAGC 60
                *****
BshCFwd      AGTGACCCTGTAAACAGGATTATTTCAATATGATGCAGCTCAACAAACTAGTTTGTAA 240
BshCaureus   AGTGACCCTGTAAACAGGATTATTTCAATATGATGCAGCTCAACAAACTAGTTTGTAA 120
                *****
BshCFwd      AAAAGGATGTCTAAAGAAAATAATGGAAGAGAAGCGGCATTAGCGAATGTTATTCGTGAA 300
BshCaureus   AAAAGGATGTCTAAAGAAAATAATGGAAGAGAAGCGGCATTAGCGAATGTTATTCGTGAA 180
                *****
BshCFwd      TATATGAGTGATTTAAAGCTTTCAAGTGAACAAGAATTAAACATACAACATTTAGCTAAT 360
BshCaureus   TATATGAGTGATTTAAAGCTTTCAAGTGAACAAGAATTAAACATACAACATTTAGCTAAT 240
                *****
BshCFwd      GGTTCAAAAGTTGTGATTGGTGGACAACAAGCAGGGCTTTTCGGGGGACCATTGTATACA 420
BshCaureus   GGTTCAAAAGTTGTGATTGGTGGACAACAAGCAGGGCTTTTCGGGGGACCATTGTATACA 300
                *****
BshCFwd      TTCCATAAAATATTTTCAATCATTACTTTATCTAAGGAATTAACGGATACACATAAGCAA 480
BshCaureus   TTCCATAAAATATTTTCAATCATTACTTTATCTAAGGAATTAACGGATACACATAAGCAA 360
                *****
BshCFwd      CAAGTAGTACCAGTTTTTTGGATTGCAGGAGAAGATCATGATTTCGATGAAGTGAATCAT 540
BshCaureus   CAAGTAGTACCAGTTTTTTGGATTGCAGGAGAAGATCATGATTTCGATGAAGTGAATCAT 420
                *****
BshCFwd      ACATTTGTTTATAACGAAAATCATGGGTCGCTGCATAAGGTTAAATATCATACAATGGAG 600
BshCaureus   ACATTTGTTTATAACGAAAATCATGGGTCGCTGCATAAGGTTAAATATCATACAATGGAG 480
                *****
BshCFwd      ATGCCAGAGACGACTGTCTCTAGATATTATCCTGATAAGGCTGAGTTGAAACAAACTTTA 660
BshCaureus   ATGCCAGAGACGACTGTCTCTAGATATTATCCTGATAAGGCTGAGTTGAAACAAACTTTA 540
                *****
BshCFwd      AAAACGATGTTTCATTTCATATGAAAGAACTGTTTCATACACAAGGTCTACTGGAGATTGT 720
BshCaureus   AAAACGATGTTTCATTTCATATGAAAGAACTGTTTCATACACAAGGTCTACTGGAGATTGT 600
                *****
BshCFwd      GACAGAATTATTGACCAATATGACTCGTGGACTGATATGTTTAAAGCACTACTGCATGAA 780
BshCaureus   GACAGAATTATTGACCAATATGACTCGTGGACTGATATGTTTAAAGCACTACTGCATGAA 660
                *****
BshCFwd      ACATTTAAAGCATATGGCGTTCTATTTATAGATGCGCAGTTTGAGCCGTTAAGAAAAATG 840
BshCaureus   ACATTTAAAGCATATGGCGTTCTATTTATAGATGCGCAGTTTGAGCCGTTAAGAAAAATG 720
                *****
BshCFwd      GAAGCGCCTATGTTTAAAAAGATTTTGAAAAACATCAGTTGCTTGATGATGCTTTTGA 900
BshCaureus   GAAGCGCCTATGTTTAAAAAGATTTTGAAAAACATCAGTTGCTTGATGATGCTTTTGA 780
                *****
BshCFwd      GCAACACANCAACGTACTCAAATCAAGGCTTGAATGCGATGATACAAACAGATACAAAT 960
BshCaureus   GCAACACACAACGTACTCAAATCAAGGCTTGAATGCGATGATACAAACAGATACAAAT 840
                *****
BshCFwd      GTTCATTTATTCTTTACATGATGAAAATATGCGTCAATTAGTTTCGTATGATGGTANGCN 1020
BshCaureus   GTTCATTTATTCTT-ACATGATGAAAATATGCGTCAATTAGTTTCGTATGATGGTAAGCA 899
                *****
BshCFwd      TTTTAAATTAATAAAACCGGATA----- 1043
BshCaureus   TTTTAAATTAATAAAACAGATAAGACATATATAAAGGAAGAAATTATAAATATTGCGGA 959
                *****
BshCFwd      -----GACCTTN----- 1050
BshCaureus   AAATCAACCTGAATTATTTTCTAATAATGTAGTGACAAGACCATTAATGGAAGAATGGTT 1019
                *****
BshCFwd      -----
BshCaureus   ATTTAACACGGTGGCATTTGTTGGAGGACCGAGTGAAATTAAGTACTGGGCTGAACTAAA 1079
BshCFwd      -----
BshCaureus   AGATGTATTTGAACTATTTGATGTTGAAATGCCTATCGTGATGCCAAGGCTTAGAATTAC 1139

```

CLUSTAL 2.1 multiple sequence alignment

```

BshCaureus    AAAACGATGTTTCATTTCATATGAAAGAACTGTTTCATACACAAGGTCTACTGGAGATTGT
BshCRev       -----CCAAATATGACTCGNGGACTGATATGTTTAAAGCNCTACTGCNTGAA 46
BshCaureus    GACAGAATTATTGACCAATATGACTCGTGGACTGATATGTTTAAAGCACTACTGCATGAA 660
               *****
BshCRev       ACCATTTAAAGCATATGGCGTTCATTTATAGATGCGCAGTTTGAGCCGTTAAGAAAAAT 106
BshCaureus    AC-ATTTAAAGCATATGGCGTTCATTTATAGATGCGCAGTTTGAGCCGTTAAGAAAAAT 719
               ** *****
BshCRev       GGAAGCGCCTATGTTTAAAAAGATTTTGAAAAACATCAGTTGCTTGATGATGCTTT-AG 165
BshCaureus    GGAAGCGCCTATGTTTAAAAAGATTTTGAAAAACATCAGTTGCTTGATGATGCTTTTAG 779
               *****
BshCRev       AGCAACACAACAACGTACTCAAATCAAGGCTTGAATGCGATGATACAAACAGATACAAA 225
BshCaureus    AGCAACACAACAACGTACTCAAATCAAGGCTTGAATGCGATGATACAAACAGATACAAA 839
               *****
BshCRev       TGTTCAATTTATTCTTACATGATGAAAATATGCGTCAATTAGTTTCGTATGATGGTAAGCA 285
BshCaureus    TGTTCAATTTATTCTTACATGATGAAAATATGCGTCAATTAGTTTCGTATGATGGTAAGCA 899
               *****
BshCRev       TTTTAAATTAATAAAACAGATAAGACATATATAAAGGAAGAAATTATAAATATTGCGGA 345
BshCaureus    TTTTAAATTAATAAAACAGATAAGACATATATAAAGGAAGAAATTATAAATATTGCGGA 959
               *****
BshCRev       AAATCAACCTGAATTATTTTCTAATAATGTAGTGACAAGACCATTAATGGAAGAATGGTT 405
BshCaureus    AAATCAACCTGAATTATTTTCTAATAATGTAGTGACAAGACCATTAATGGAAGAATGGTT 1019
               *****
BshCRev       ATTTAACACGGTGGCATTGTTGGAGGACCGAGTGAAATTAAGTACTGGGCTGAACATAA 465
BshCaureus    ATTTAACACGGTGGCATTGTTGGAGGACCGAGTGAAATTAAGTACTGGGCTGAACATAA 1079
               *****
BshCRev       AGATGTATTTGAACTATTTGATGTTGAAATGCCTATCGTGATGCCAAGGCTTAGAATTAC 525
BshCaureus    AGATGTATTTGAACTATTTGATGTTGAAATGCCTATCGTGATGCCAAGGCTTAGAATTAC 1139
               *****
BshCRev       TTATTTAAATGACCGTATAGAAAAATTACTTTGAAATACAATATTCCATTAGAAAAAGT 585
BshCaureus    TTATTTAAATGACCGTATAGAAAAATTACTTTGAAATACAATATTCCATTAGAAAAAGT 1199
               *****
BshCRev       GTTAGTCGATGGTGTGGAAGGAGAAAGAAGTAAGTTTATTAGAGAACAAGCATCACATCA 645
BshCaureus    GTTAGTCGATGGTGTGGAAGGAGAAAGAAGTAAGTTTATTAGAGAACAAGCATCACATCA 1259
               *****
BshCRev       ATTTATTGAAAAGGTAGAAGGTATGATTGAACAACAGCGTCGTCTAAACAAAGACTTATT 705
BshCaureus    ATTTATTGAAAAGGTAGAAGGTATGATTGAACAACAGCGTCGTCTAAACAAAGACTTATT 1319
               *****
BshCRev       AGATGAAGTGGCGGGAATCAAATAATATTAACCTTGTGAATAAAAATAATGAAATTCA 765
BshCaureus    AGATGAAGTGGCGGGAATCAAATAATATTAACCTTGTGAATAAAAATAATGAAATTCA 1379
               *****
BshCRev       TATACAACAGTATGATTATTTGTTAAAACGTTATCTTTTAAACATTGAAAGAGAAAACGA 825
BshCaureus    TATACAACAGTATGATTATTTGTTAAAACGTTATCTTTTAAACATTGAAAGAGAAAACGA 1439
               *****
BshCRev       CATCAGTATGAAGCAATTTAGAGAAATTCAAGAAACACTCCATCCAATGGGAGGATTACA 885
BshCaureus    CATCAGTATGAAGCAATTTAGAGAAATTCAAGAAACACTCCATCCAATGGGAGGATTACA 1499
               *****
BshCRev       AGAAAGAATATGGAATCCACTTCAAATTTTGAATGATTTTGGGACAGATGTGTTCAAGCC 945
BshCaureus    AGAAAGAATATGGAATCCACTTCAAATTTTGAATGATTTTGGGACAGATGTGTTCAAGCC 1559
               *****
BshCRev       CTCCACCTATCCACCCTTTCTTACACTTTTGATCATATTATTATAAAACCTTAACCTGA 1005
BshCaureus    CTCCACCTATCCACCCTTTCTTACACTTTTGATCATATTATTATAAAACCTTAA----- 1614
               *****
BshCRev       GCACCACCACCACCACCTGAGATCCGGCTGCTACAAGCCCGAAGGAGNAG 1057
BshCaureus    -----

```

Consensus key: * :single, fully conserved residue - : no consensus

Figure 7. Sequence Alignment of BshC *S. aureus*. Sequence of the PCR product was aligned to the known WT sequence of *S. aureus* BshC using ClustalW for both the sequence from the T7 forward primer and the complement of the sequence from the reverse primer.

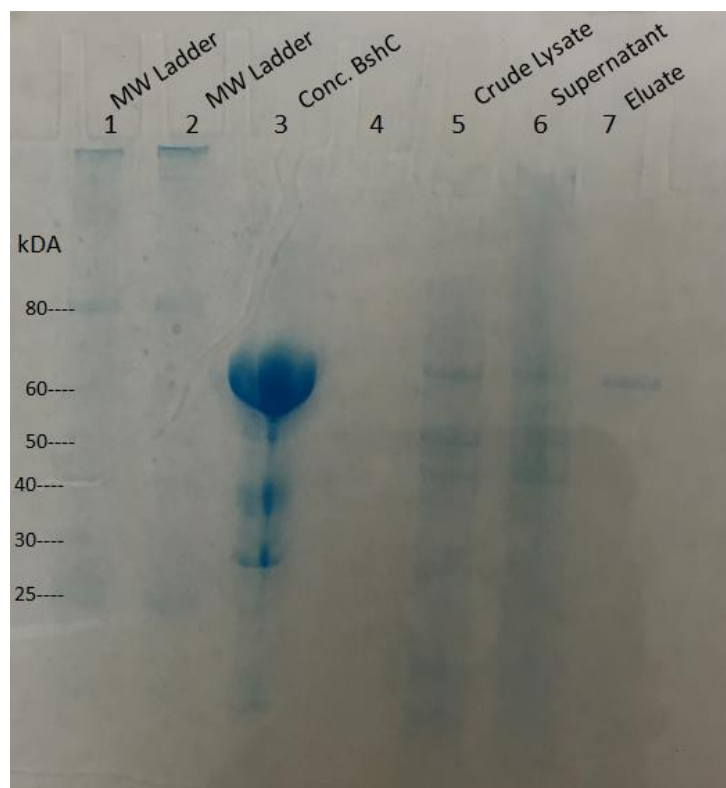


Figure 8. BshC Solubility Expression SDS-PAGE. SDS-PAGE on small scale protein expression of BshC *S. aureus*, and subsequent large scale, was used to assess expression, solubility, and purity.

Expression and purity of BshC protein was tested on a small scale and analyzed by SDS-PAGE in Figure 8. The ladder is very faint in lanes 1 and 2 but MW bands are still legible. Lanes 5 and 6 show soluble proteins in the lysate and supernatant. Both of these lanes have many bands, evidence of many different proteins present. Lane 7, however, only contains one band at 62kDa which is the estimated MW of BshC *S. aureus*. BshC protein was successfully purified as evidenced by the single band in lane 7. Lane 3 shows the result of affinity chromatography on a large scale. It can be concluded that the protein is pure because there is such a strong signal of BshC present when compared to the potential contaminating bands. Too much concentrated protein was loaded and next time loading less volume would give a more accurate assessment of purity. rTEV was successfully used to cleave the his-tag from the protein as determined qualitatively by Bradford assay.

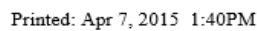
Despite a multitude of crystallization screens, no BshC *S. aureus* protein crystals have yet been grown. At this point, no actual x-ray crystallographic data was able to be collected. Therefore, the model predicted by *PHYRE2* is currently the best model available. The idea that BshC from

S. aureus may not bind ADP is currently being tested by obtaining a crystal structure which accurately reflects protein structure. *In vitro* assays of BshC *B. subtilis* were analyzed by HPLC analysis with substrates cysteine, glucosaminyl-malate, and either ATP, CTP, GTP, NADH, Zn^{2+} with ATP, or serine with ATP. Assays were also performed on BshC *S. aureus* with cysteine, glucosaminyl-malate, and ATP. The results did not reveal any enzyme activity. The HPLC trace for BshC with NADH had an unidentifiable peak detected at 4.681 minutes. Future work is needed to characterize this finding. Employing x-ray crystallography to understand how the structure of BshC dictates its function will allow specific inhibitors to be designed that stop bacillithiol biosynthesis. The absence of bacillithiol will allow fosfomycin to be re-established as an effective antibiotic once again.

References

1. Gaballa, A.; Newton, G.; Antelmann, H.; Pasonage, D.; Upton, H.; Rawat, M.; Claiborne, A.; Fahey, R.; Helmann, D. Biosynthesis and functions of bacillithiol, a major low-molecular-weight thiol in *Bacilli*. PNAS 2010, 107, 6482-6486.
2. Parsonage, D., Newton, G.L., Holder, R.C., Wallace, B.D., Paige, C., Hamilton, C.J., Dos Santos, P.C., Redinbo, M.R., Reid, S.D. and Claiborne, A. (2010) Characterization of the N-acetyl-a-D-glucosaminyl L-malate synthase and deacetylase functions for bacillithiol biosynthesis in *Bacillus anthracis*. Biochemistry 49, 8398–8414.
3. Patel, S.; Balfour, J.; Bryson, H. Fosfomycin tromethamine: A review of its antibacterial activity, pharmacokinetic properties, and therapeutic efficacy as a single-dose oral treatment for uncomplicated lower urinary tract infections. Drugs 1997, 53, 637-656.
4. Tang, H.; Chen, C.; Cheng, K.; Toh, H.; Su, B.; Chiang, S.; Ko, W.; Chuang, Y. In vitro efficacy of fosfomycin-containing regimens against methicillin-resistant *Staphylococcus aureus* in biofilms. J. Antimicrob. Chemother. 2012, 67, 944-950.
5. Thompson, M.; Keithly, M.; Harp, J.; Cook, P.; Jagessar, K.; Sulikowski, G.; Armstrong, R. Structural and chemical aspects of resistance to the antibiotic fosfomycin conferred by FosB from *Bacillus cereus*. Biochemistry 2013, E-pub ahead of print.
6. Lamers, A.; Keithly, M.; Kim, K.; Cook, P.; Stec, D.; Hines, K.; Sulikowski, G.; Armstrong, R. Synthesis of bacillithiol and the catalytic selectivity of FosB-type fosfomycin resistance proteins. Organic Letters 2012, 14, 5207-5209.
7. Upton, H.; Newton, G.; Gushiken, M.; Lo, K.; Holden, D.; Fahey, R.; Rawat, M. Characterization of BshA, bacillithiol glycosyltransferase from *Staphylococcus aureus* and *Bacillus anthracis*. FEBS Letters . 2012, 586, 1004-1008.
8. Fan, F., Luxenburger, A., Painter, G. F., and Blanchard, J. S. (2007) Steady-state and pre-steady-state kinetic analysis of *Mycobacterium smegmatis* cysteine ligase (MshC), Biochemistry 46, 11421-11429.
9. VanDuinen, A.J., Winchell, K.R., Keithly, M.E., Cook, P.D. X-ray Crystallographic Structure of BshC, a Unique Enzyme Involved in Bacillithiol Biosynthesis. Biochemistry 2015, 54: 100-103

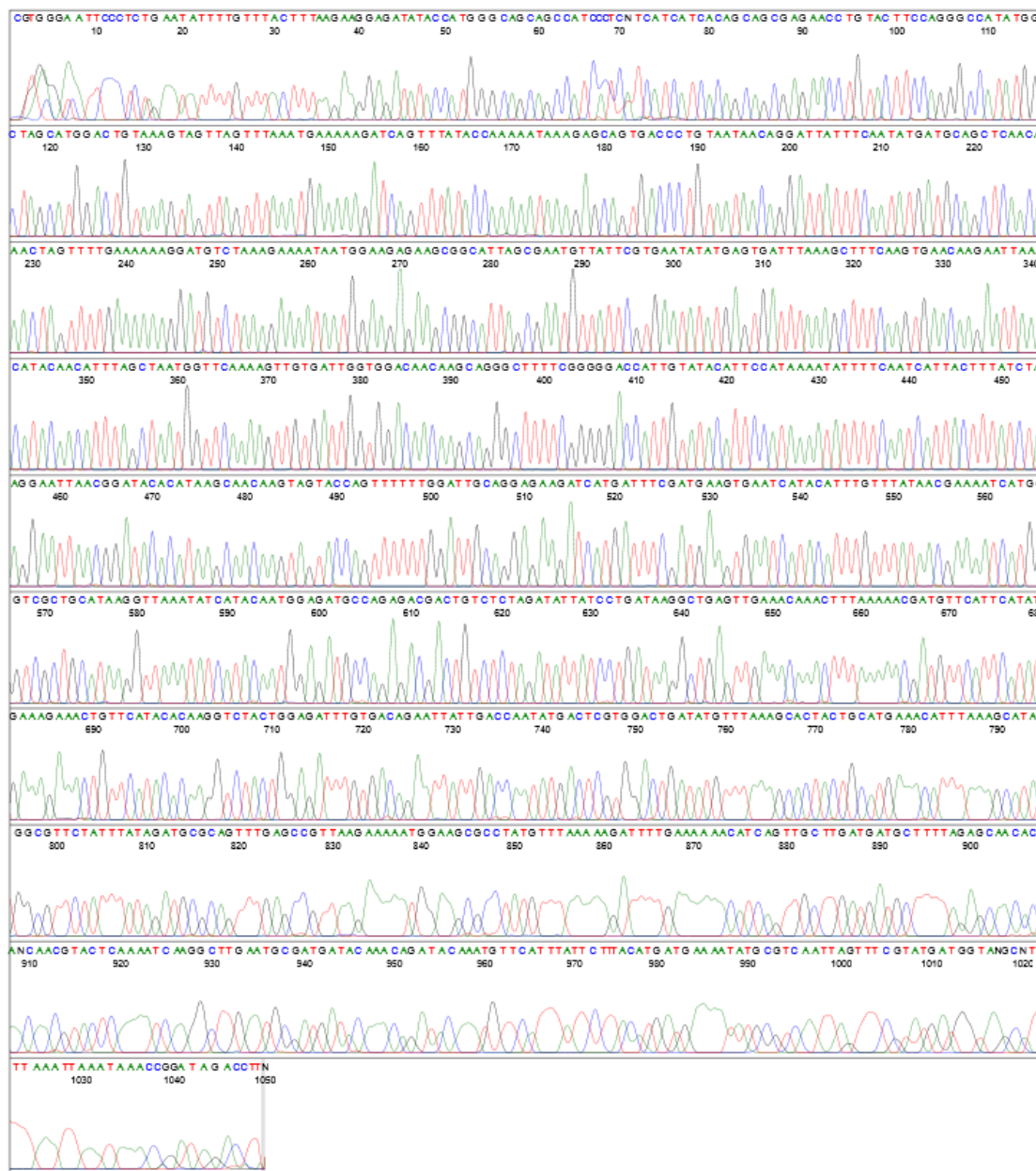
Supplemental Figure 1. Chromatogram from Forward Primer. Chromatogram produced by DNA sequencing PCR product with the T7 forward primer.



File: 2424422_T7.ab1

Sample Name: 2424422.T7
Mobility: DT3730POP7{BDv3}.mob
Spacing: 14.03
Comment: sPDC023_{paul_cook}

Signal Strengths: A = 910, C = 461, G = 635, T = 837
Lane/Cap#: 18
Matrix: n/a
Direction: Native



Printed: Apr 7, 2015 2:51PM

FinchTV v.1.4.0

Page 1 of 1

Supplemental Figure 2. Chromatogram from Reverse Primer. Chromatogram produced by DNA sequencing PCR product for the reverse primer.